

Optimal Control for Rotors with Circulating Forces due to Spinning Dissipation

A. Mukherjee^{1*}, S. Sengupta²

¹ Assistant Professor, Department of Applied Electronics and Instrumentation engineering, National Institute of Science and Technology, Berhampur, Palur Hills, Orissa, India

² Professor, Department of Electrical Engineering, Indian Institute of Technology, Kharagpur, West Bengal India

* Corresponding author (email: abhro456@gmail.com)

Abstract

Rotors at speeds higher than certain threshold values become unstable due to rotating damping forces generated by dissipation in rotor material, couplings or due to friction in splines and tool tips. There are several techniques by which one may stabilize such rotors. Although the current methods in practice are quite effective for large or medium size rotors but these may not be suitable for small, mini or micro rotor systems. This paper proposes a class of alternative techniques to stabilize such small size rotors.

This work reveals some interesting facts. For rotors without torsional load the shaft drawn power entirely goes for only fostering whirling motion. The power may be used for modulating contrived negative rotating damping to stabilize the rotor. But for rotors having torsional loads, the shaft drawn power would be more than needed only to sustain whirling motion and thus may cause over reduction of effective rotating damping and the shaft would then eventually whirl in reverse direction with rapidly growing whirl amplitude and would be unstable.

Two alternative approaches of using orbital response functions are proposed which are created by measurement of orthogonal vibration velocity amplitude in frame rotating with the shaft and the actively contrive negative rotating dampers are modulated with suitable functions these signals. It has been shown in this paper that by such improvisations of modulations the negative damping coefficients stabilize the shaft for both with added eccentricity and with torsional load or their combination. The stabilizing scheme may be implemented with in a suitably designed coupling between the rotor and its drive.

Keywords: Rotating dampers, non-potential forces, Bond-graphs, regenerative power (Shaft Drawn Power),

Threshold spinning speed, SPBF (Shaft Power Bounding Function), whirl orbital response functions.

1 Introduction

Dynamical systems subjected to such displacement dependent forces, not derivable from gradient of potential functions may become unstable. Such non-potential forces may develop due to dissipative forces rotating with the spinning system. The destabilizing effects of dissipative forces in cases of topes and pendulums like system have been studied by Bou-Rabee, Marsden and Romero [1], Kirillov [2], Or [3], Samantaray et al [4]. These forces may import energy from the drives or other exogenous sources or even kinetic energy of inertial part causing instability. Some significant examples of such engineering systems are elastic rotors with internal or material damping forces or dissipative forces in couplings, hydrodynamic forces due to bearings supporting the rotor and elastic structures subjected to aerodynamic forces. Several efforts to study dynamics of such systems and the proposals for their stabilization are reported in literature [5, 6]. These proposals are mainly passive in nature such as incorporating additional environmental dissipation as in case of rotors with deploying squeeze film dampers [7, 8], suspended visco-elastic particles in the lubricating mediums[9, 10,11] or incorporation of dissipative seethes on aero-elastic structures. In case of rotors these stabilizing techniques may be deployed on for large or medium size rotors.

This paper is devoted to study on such system i.e. rotors with rotating dissipation. Efforts have also been made to create efficient controllers to stabilize these rotors and it has been also ensured that these controllers are practically realizable. The technique proposed here may be implemented in small, mini or micro size rotors.

A brief discussion on non-potential force field due to spinning dissipation is incorporated. For detailed discussion on this aspect reader may see reference [12].

After establishing the non-potential nature of rotating dampers, bond graph models of pendulum rotors with spinning dampers are created. Bond graphs facilitate creation of holistic dynamical system belonging to multi-energy domain. Piezo and electromagnetic actuators have been used in the models as final controlling element. The modeling of spinning shaft with embedded smart structures in rotating frames incorporated the coupling between drive and rotor is created for several stabilizing strategies. Practical issues like shaft eccentricity and loads are also considered in the model. To obtain a relatively robust control law the dependence of threshold spinning speeds of the shaft beyond which the shafts get destabilized is analyzed. It can be theoretically shown that the active stabilization of the shaft can be achieved by altering the shaft's stationary damping, rotating or material damping or shaft natural frequency by active control. Arguments have been presented in sequel in the paper in favor of the final choice proposed. It has been shown that practical stabilization can be achieved by active alteration of rotating damping, which may be realized using the embedded piezo or electromagnetic actuators in the smart coupler. We have also taken special efforts to develop a thorough theoretical control strategy to ensure an complete stabilization of the rotor. We have discussed the effectiveness of the control algorithm by showing its path by considering its convergence through Bounding Function. Spatial trajectory and regions of the bounding function is shown for absolutely no delay, small delay and large delay conditions. We have also proposed a smart structure coupling embedded within the shaft-rotor system to make it practically realizable. The entire idea is validated by computer simulation whose results are appended within the later sections of the paper. Symbols Shakti version 2.0.1[13] Software has been used for modeling and simulation.

2 Analysis of Spinning Systems with External and Internal or Material Damping

Consider a system with mass and internal damping (isotropic) only

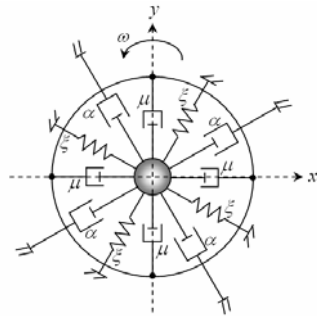


Fig 1: Schematic Representation of Fixed and Rotational Dampers.

The aerial damping coefficient is taken as $\alpha = R_a/2$, such that effective damping coefficient in all direction is R_a . Likewise frame is taken as $\mu = R_i/2$, such that its

effective value in all direction is R_i . The stiffness is assumed to be $\xi = K_s/2$, such that stiffness K_s is experienced in all directions. See ref. [12].

The rotating damping forces act in the frame rotating along with the dampers. The velocity in the rotating frame are related to those in fixed frame in co-oriented coordinate as follows (i, j, k are the unit vectors).

$$V_f = V_r + \omega \times r,$$

$$\begin{aligned} V_f &= V_r + \omega_k \times (x_i + y_j), \\ &= V_r + \omega y_i - \omega x_j \end{aligned} \quad (1)$$

In matrix notations

$$\begin{bmatrix} V_{x,f} \\ V_{y,f} \end{bmatrix} = \begin{bmatrix} V_{x,r} \\ V_{y,r} \end{bmatrix} + \begin{bmatrix} 0 & \omega \\ -\omega & 0 \end{bmatrix} \begin{bmatrix} X \\ Y \end{bmatrix} \quad (2)$$

In terms of displacement components

$$\begin{bmatrix} \dot{X}_r \\ \dot{Y}_r \end{bmatrix} = \begin{bmatrix} \dot{X}_f \\ \dot{Y}_f \end{bmatrix} + \begin{bmatrix} 0 & -\omega \\ \omega & 0 \end{bmatrix} \begin{bmatrix} X \\ Y \end{bmatrix} \quad (3)$$

The force vector would be,

$$\begin{bmatrix} F_x \\ F_y \end{bmatrix} = R_i \begin{bmatrix} \dot{X}_f \\ \dot{Y}_f \end{bmatrix} + \begin{bmatrix} 0 & -\omega R_i \\ \omega R_i & 0 \end{bmatrix} \begin{bmatrix} X_f \\ Y_f \end{bmatrix} \quad (4)$$

The first term on the right hand side is like ordinary damping force where as the second term has special features which will be discussed below. This component of the force will be called as circulating force due to reasons which will be shown later in the paper.

Let us consider the circulating component of the force vector,

$$\begin{bmatrix} F_x \\ F_y \end{bmatrix} = \begin{bmatrix} 0 & -\omega R_i \\ \omega R_i & 0 \end{bmatrix} \begin{bmatrix} X \\ Y \end{bmatrix} \quad (5)$$

In vector notations the circulating force, \bar{F}_c , may be written as,

$$\bar{F}_c = -\omega R_i \hat{Y} + \omega R_i \hat{X} \quad (6)$$

Where \hat{i} and \hat{j} are unit vectors in X and Y directions.

The special features of this force can not be derived from a potential function i.e. $\bar{F}_c \neq -\nabla\phi$ for any function $\phi(X, Y)$.

This may be proved by the fact that it has non-vanishing curl,

$$\nabla \times \bar{F}_c = \left(\frac{\partial}{\partial X_i} \hat{i} + \frac{\partial}{\partial Y_j} \hat{j} \right) \times (-\omega R_i \hat{Y} + \omega R_i \hat{X}) = 2\omega R_i \hat{k} \quad (7)$$

With $\hat{k} = \hat{i} \times \hat{j}$.

This has a significant implication as the work done by the force \bar{F}_c will be path dependent. In other words it will do net work when the point of application traces a closed orbit. Say the point is moved in a circular orbit around its equilibrium point at $X = Y = 0$ then work done in such on orbit will be

$$\begin{aligned} W_c &= \oint \bar{F}_c \cdot d\bar{r} = \iint (\nabla \times \bar{F}_c) \cdot d\bar{a} \\ &= \iint 2\omega R_i \hat{k} \cdot d\hat{a} \\ &= 2\omega R_i A \end{aligned} \quad (8)$$

Here A is the area of the orbit.
If the circulating force vector is a nonlinear function of position vector $F_C = \omega f(x, y)$.

$$\text{Then } W_C = \omega \nabla \times f(x, y) \cdot A_k \quad (9)$$

And the entire preceding argument will be valid except that W_C is not proportional to the area but will have somewhat complex dependencies.

In this paper we have considered linear internal damping.

3 Theoretical Analysis of Strategies used for Active Stabilization of a single degree of freedom Rotor.

3.1 Determination of Instability Threshold Spinning Speed

We need to find out the critical spinning speed beyond which the system becomes practically unstable.

Regenerative work per orbit as stated earlier $W_C = 2\omega R_i A$, for a circular orbit (the system symmetry suggests that this orbit has to be circular).

$A = \pi r^2$, where r is the radius of the orbit. $W_C = 2\pi\omega R_i r^2$. The dissipative work done due to damping ($R_a + R_i$) would be

$$W_d = (2\pi r) * (\omega_n r) * (R_a + R_i). \quad (10)$$

Now at balanced condition the regenerative power will be almost nearing the dissipative power therefore the condition $W_C = W_d$. We get the same relation that is $\omega_{th} = \omega_n (1 + R_a / R_i)$. We can denote this threshold spinning speed by ω_{th} . At speed $\omega > \omega_{th}$ the regenerative energy per orbit or regenerative power will be larger than power dissipated by damping $R_a + R_i$. The system will become unstable and there will be continuous growth of the power drawn from the drive as will be shown later section by the simulation results.

It has been observed that the critical spinning speed depends on the shaft natural frequency, the external damping and also rotating damping. Therefore it is possible to achieve stability by increasing the value of ω_{th} (refer to the relation $\omega_{th} = \omega_n (1 + R_a / R_i)$).

3.2 Limitations of Stabilizing Control by the Shaft Natural Frequency & Shaft Stationary Damping

Keeping rotor inertial unchanged one may increase shaft stiffness by feeding back shaft displacement. Often this way of stabilization would technically be difficult and there would be limits up to which the stiffness could be increased in flexible rotors with limited number of actuators. Therefore it would not be a practical proposition to handle the shaft natural frequency in order to stabilize the shaft.

Increasing the shaft stationary damping R_a is another way by which we could shift the shaft critical speed and stabilize but there may be certain limitations in this approach too. By applying velocity proportional force in stationary frame on the shaft one may artificially increase R_a . This will lead to increase in ω_{th} . However, depending on the range $\omega - \omega_{th}$, the difference of spinning and the instability onset speed the feedback gains will have to be increased. For larger differences of these speed larger gain would be needed. This would certainly mean a larger actuation problem. In addition to this for application of these forces a rigid stationary structure would be needed which may not be practically implemented with the rotating shaft. There would be severe constraints and problems to integrate such systems with the rotating shaft. There may also be additional problems arising to implement such systems due to high contact friction and wear in the actuators.

3.3 Control of spinning rotors with active modification of rotating dampers

If we recall the relation of the instability threshold speed $\omega_{th} = \omega_n (1 + R_a / R_i)$, the R_i appears in the denominator which determines the internal damping or damping in rotating frame. Now if by control action, that is by feeding back the forces proportional to the velocities in rotating frame the effective internal damping, may be reduced. This will lead to high values of ω_{th} . One may say $R_{eqv} = R_i - R_c$, where R_{eqv} is the effective value of rotating damping. Original material damping and R_c is the negative damping created by the control action. With this control the effective ω_{th} would be

$$\omega_{th} = \omega_n (1 + R_a / (R_i - R_c)) = \omega_n (1 + R_a / R_{eqv}). \quad (11)$$

This control has several advantages

- This has to be implemented in a frame rotating with the shaft or on the shaft itself. Thus this method of smart structures may be effectively used. Piezo actuators, PZT's, electro-magnetic devices. Electromagnetic devices in rotating frames may be used for relatively larger rotors.
- As the limit of R_c is from 0 to R_i for whole range of spinning speeds the gain values and controller actuation forces are also limited and it does not reach a very high unacceptable values.

3.4 Development of the Control Law and Determination of the Bounding Function

It has been shown later in the paper that the shaft drawn power monotonically increases when the shaft becomes unstable. Thus in design of R_C the shaft drawn power from the drive from would be used as follows:

$$R_C = \alpha P + \beta t \int_0^t P(\varepsilon) d\varepsilon + \sigma dP/dt \quad (12)$$

The shaft drawn energy per orbit would be

$$W_{EC} = 2\omega R_{eqv} A = 2\omega R_{eqv} \pi r^2 \quad (13)$$

where r is radius of the orbit.

The shaft center at a speed ω_n rad/sec and the radius of the shaft is r . The time of one orbit in $T = 2\pi/\omega_n$. The shaft power drawn would be

$$P_C = W_{EC}/T = 2\omega R_{eqv} \pi r^2 / 2\pi/\omega_n = \omega \omega_n r^2 R_{eqv} \quad (14)$$

The dissipative work per orbit is

$$W_D = \omega_n r (R_a + R_{eqv}) * 2\pi r \quad (15)$$

$$= 2\pi r^2 \omega_n (R_a + R_{eqv}) \quad (16)$$

Thus dissipative power would be

$$P_D = W_D/T = r^2 \omega_n^2 (R_a + R_{eqv}) \quad (17)$$

Now if one assumes at instability the mass centre trajectory spirals out at a rate much slower rate than the orbiting frequency of the shaft. The shaft power relation may be written as

$$\omega \omega_n r^2 R_{eqv} = \omega \omega_n r^2 ((R_i - \alpha P - \beta \int_0^t P(\varepsilon) d\varepsilon - \sigma dP/dt) = P \quad (18)$$

The dissipative power is less than regenerative or shaft power drawn which is given by the condition

$$r^2 \omega_n^2 (R_a + R_{eqv}) < P \quad (19)$$

Here it is assumed that the shaft is already in unstable range.

$$\omega_n^2 r^2 (R_a + R_i - \alpha P - \beta \int_0^t P(\varepsilon) d\varepsilon) - \sigma dP/dt < P \quad (20)$$

Or

$$\omega_n r^2 < P / (\omega_n (R_a + R_i - \alpha P - \beta \int_0^t P(\varepsilon) d\varepsilon - \sigma dP/dt)) \quad (21)$$

The above inequality may be arrange as,

$$R_i (\omega - \omega_{in}) / (\omega - \omega_n) \geq (\alpha P + \beta \int_0^t P d\varepsilon + \sigma dP/dt) \quad (22)$$

Taking Laplace transform of both sides, rearranging the equation and then taking Laplace inverse transform one obtains.

From the above relation we obtain

$$\mathcal{L}^{-1} \left[\frac{\{R_i (\omega - \omega_{in}) / (\omega - \omega_n) + \beta P(0)s\}}{\beta (\sigma s^2 + \alpha s + \beta)} \right] \geq P(t) \quad (23)$$

Where $\mathcal{L}^{-1}()$ Laplace inverse transform and $P(0)$ is the value of shaft power drawn at time when controller is switched on. As the system is time invariant this time may be taken as $t = 0$.

We denote $R_i (\omega - \omega_{in}) / \sigma (\omega - \omega_n) = \sigma$

and $\beta / \sigma = \beta^*$, $\alpha^* = \alpha / \sigma$.

Therefore the inequality transforms to

$$\mathcal{L}^{-1} \left[\frac{(\sigma + \beta^* P(0)s)}{(s^2 + \alpha^* s + \beta^*)} \right] \geq P(t) \quad (24)$$

It is further assumed that the rotor draws power from the drive and never sends it back. In other words rotor is always passive when seen from the drive port.

Denoting $\mathcal{L}^{-1} \left[\frac{(\sigma + \beta^* P(0)s)}{(s^2 + \alpha^* s + \beta^*)} \right] \equiv F_B(t)$,

$F_B(t)$ will be called Shaft Power Bounding Function (SPBF). the final inequality condition will be

$$F_B(t) \geq P(t) \geq 0.$$

The requirement is $F_B(t)$ should never be negative. Thus the parameters σ, α, β should be adjusted to meet this condition and such that the rotor is stabilized.

The condition is as $t \rightarrow \infty$ $F_a(t) \rightarrow 0$ such that the bounding function never becomes negative it may be proposed that the selection of σ, α, β be such that both

the roots of polynomial equations, $s^2 + \alpha^* s + \beta^* = 0$ are negative real. Say roots are $-\phi_1$ and $-\phi_2$ with $\theta_2 > \theta_1$

The bounding function is

$$F_B(t) = e^{-\phi_1 t} / (\phi_2 - \phi_1) \{ \rho (1 - e^{-(\phi_2 - \phi_1)t}) + \beta^* P(0) (\phi_2 e^{-\alpha t} - \phi_1) \} \quad (25)$$

The nature of this bounding function is very crucial to the stabilization of the rotor through drawn power modulation.

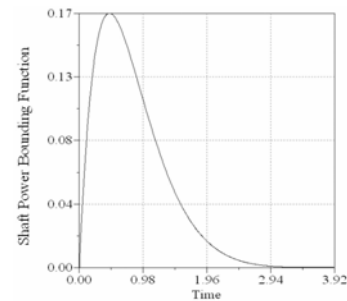


Fig 2: Variation of shaft power bounding function without starting delay with time.

4 Deployment of Piezo Structures as Actuating Element for Stabilization of a SDF Pendulum Rotor with Smart Coupling.

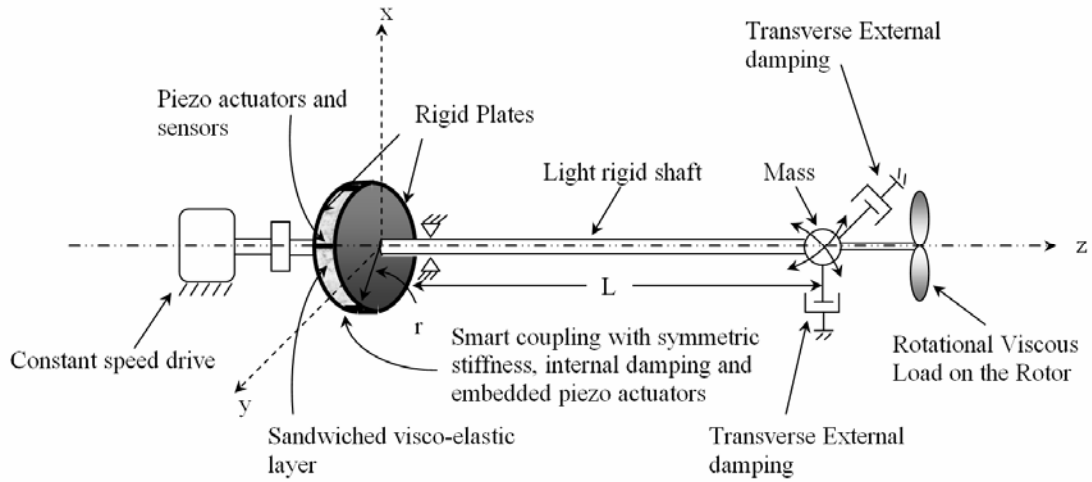


Fig 3: Single degree of freedom pendulum rotor with smart coupling.

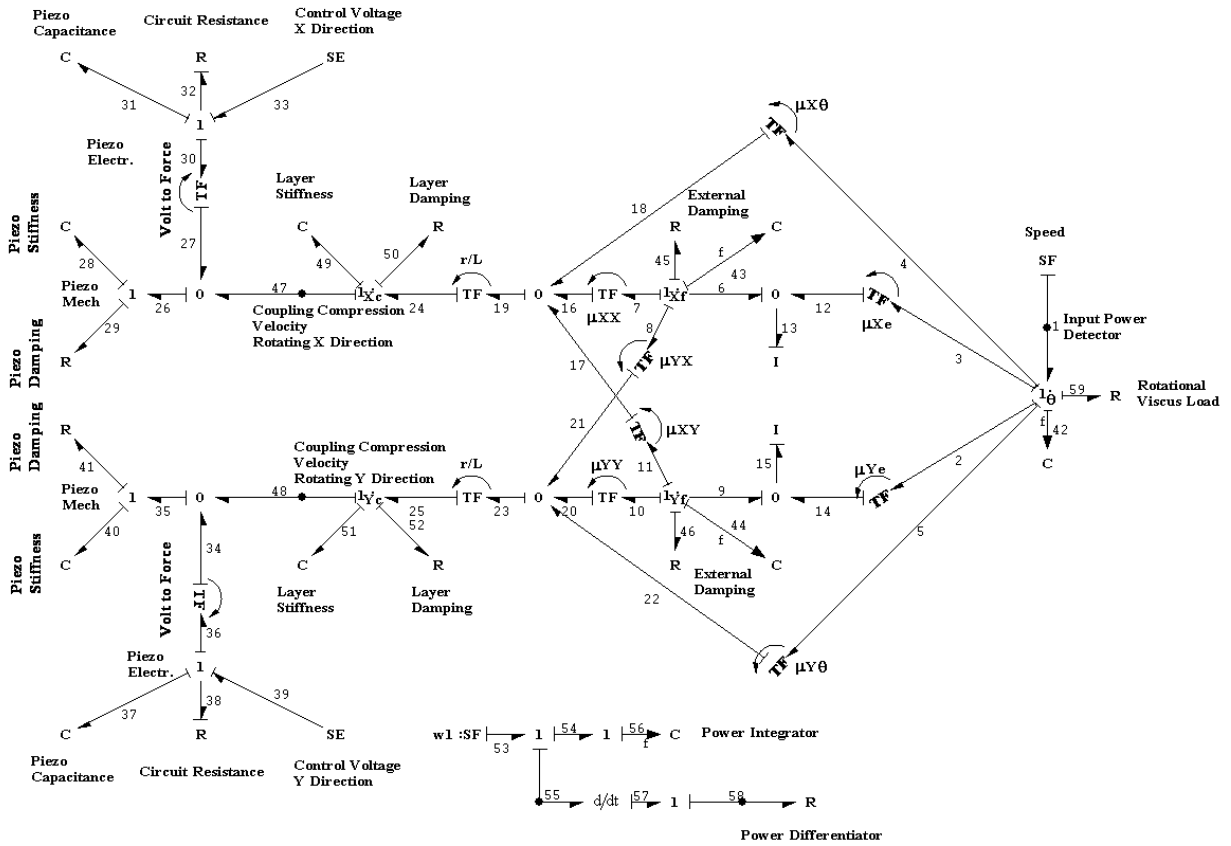


Fig 4: Bond graph model of single degree of freedom pendulum rotor with smart coupling.

A simple single degree of freedom system paradigm as shown in fig 3 is considered. This system has all the essential features which are to be addressed. It comprises of a pendulum like rotor. The external dampers are directly attached to the mass in two orthogonal directions in the fixed frame. Isotropic stiffness and internal damping rotating with the rotor are lumped in the flexible coupling connecting the constant speed drive and the rotor, just before a self aligning bearing supporting the rotor without applying any couple. The sensing and actuating elements are embedded in the coupling. These elements sense the motion and apply negative velocity proportional forces with suitable gain modulation in two orthogonal directions in a frame rotating with the rotor. The sensing and actuating elements may be realized by deployment of set of piezo crystals.

While simulating the complete system the piezo-electric constant are taken to be roughly $650 \times 10^{-12} C/N$, elastic compliance at around $20 \times 10^{-12} m^2/N$. Output impedance of roughly 500ohms, damping coefficient roughly $D_e = 20144 N/sec$ and permittivity constant $\epsilon = 5.53 \times 10^{14}$ are used for simulations. The control voltages applied across the piezo actuators are as follows.

$$V_x = V_{cap}x - R'_c * \dot{X}_r * r/L, \text{ and}$$

$$V_y = V_{cap}y - R'_c * \dot{Y}_r * r/L.$$

$$\text{Where, } R'_c = (\alpha * P + \beta * \int_0^t P dt + \sigma * dp/dt).$$

The physical value of R_c described earlier is related to R'_c as $R_c = R'_c * \zeta$ where ζ is voltage to force characteristics of the actuating crystals. $V_{cap}x$ and $V_{cap}y$ are the voltages across the capacitors. These are estimated using crystal parameters. $\dot{X}_r * r/L$ and $\dot{Y}_r * r/L$ are the X and Y components velocities as sensed by the embedded velocity sensors along with piezo actuators in the smart stabilizing coupling.

4.1 Simulation with eccentricity but no shaft load.

In this set of simulations the shaft has eccentricity of $1.0 \times 10^{-4}m$. The shaft however, does not have any rotational viscous load. The fig 5(a) shows X-velocity amplitude in fixed frame where as fig 5(b) shows the X-velocity amplitude in rotating frame as seen by the stabilizing smart coupling. In the fixed frame the vibration amplitude settles with residual amplitude. This is due to unbalance response of the rotor. In the rotating frame the velocity amplitude settles to zero as in this frame the unbalance component of velocity is not visible. This is a very significant observation. This shows that the presence of unbalance does not interfere with the active stabilization of the rotor. Figures 5(c) and 5(d) show the actual and average shaft power drawn by the rotor.

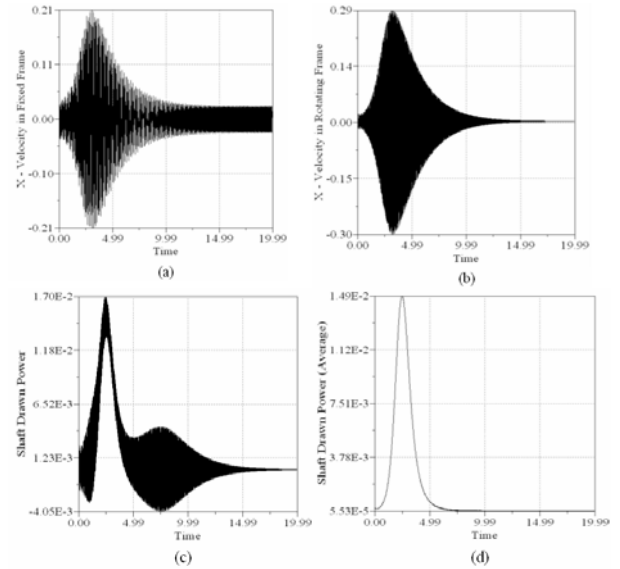
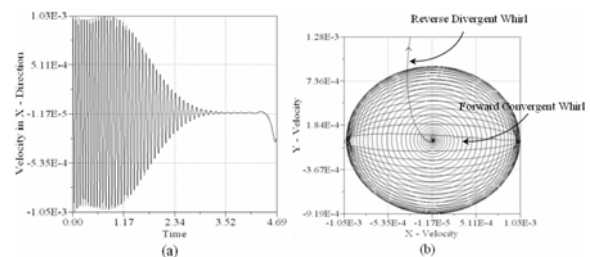


Fig 5: Dynamic response of stabilized pendulum rotor with eccentricity only

4.2 Perfectly balanced shaft with load.

For a perfectly (with no eccentricity) the shaft power drawn is sum of the power which fosters the whirling motion and the power needed by the load. Thus power drawn is more than the required towards whirling motion. Consequence of this is that R_c keeps growing even if the shaft amplitudes of vibration for whirl have reached nearly zero value. Eventually R_c becomes larger than the internal damping R_i and R_{eqv} becomes negative leading to the occurrence of eventual reverse whirl which then rapidly grows in amplitude. Shaft again becomes unstable. Following simulation results show various aspects of this phenomenon. It may be noted that the rotational viscous load on the rotor is extremely small, $R_i = 8.0 \times 10^{-7} Nms$. The power drawn by the shaft is presented in two consecutive time durations. The fig. 6(c) shows the initial phase till the onset of reversed whirl. The fig 6(d) shows a period after that when power acquires negative value and grows. The eventual buildup of negative power means power going from shaft to drive. This power comes from the actuator circuit, loading the actuating elements which may lead to their damage.



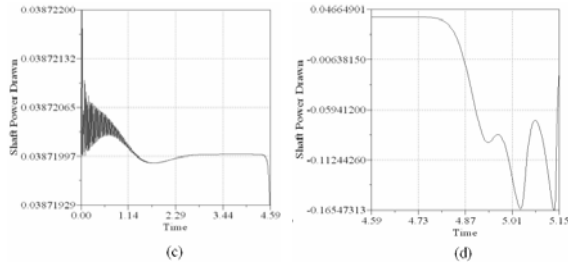


Fig 6: Dynamic response of stabilized pendulum rotor with shaft load only.

5 Stabilization by whirl orbital response functions.

For stabilization under all situations viz. rotor with unbalance and more significantly with shaft load R_c should be determined by some response function which is related to power going for whirling motion only and which is not at all related to power which is rendered to the shaft load. The orbit area is one such response function. However for practical implementation orbit radius in rotating frame i.e. $X_r^2 + Y_r^2$ as the whirl orbits are circular with slowly varying radius in rotating frame. Even better response function would be $\dot{X}_r^2 + \dot{Y}_r^2$ as the whirl orbiting speed is the natural frequency of shaft without any damping.

In the following simulations this function is implemented by taking,

$$R_c' = (\alpha * V_{amp}^2 + \beta * \int_0^t V_{amp}^2 dt + \sigma * dV_{amp}^2 / dt) \quad ,$$

$$\text{where } V_{amp}^2 = (\dot{X}_r * r/L)^2 + (\dot{Y}_r * r/L)^2.$$

The Fig. 7 shows the vibration amplitudes in fixed and rotating frames for balance shaft with relatively large shaft load, $R_1=0.02$ Nms. This strategy stabilizes the rotor even with such shaft load as expected. The power drawn by the shaft fluctuates about the load delivered to the load and then settles at this value once the whirl is stabilized.

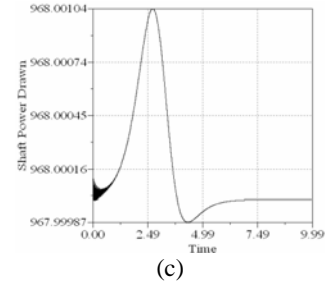
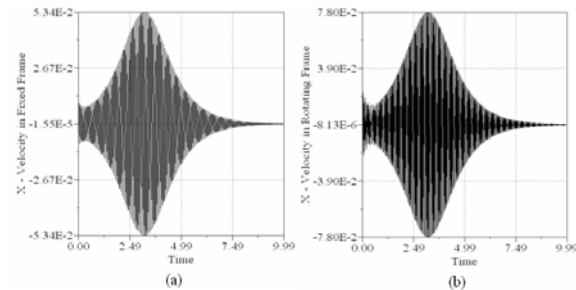


Fig 7: Dynamic response of pendulum stabilized with orbit response function-1 rotor with shaft load only.

The fig. 8 shows the response of the same shaft with eccentricity of $1.0 * 10^{-4}$ with this proposed stabilizing strategy. This is an extremely satisfactory dynamic behavior of the rotor.

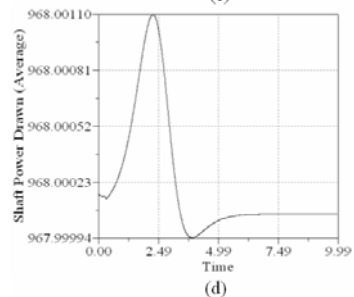
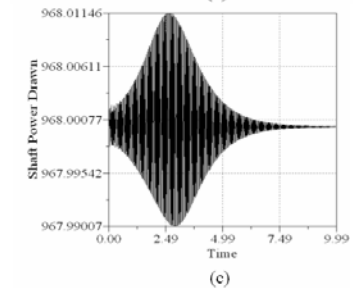
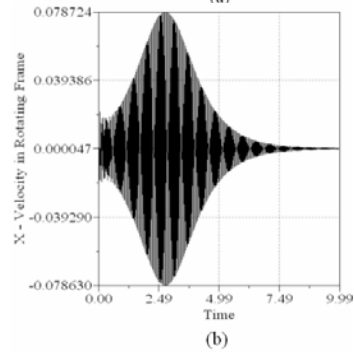
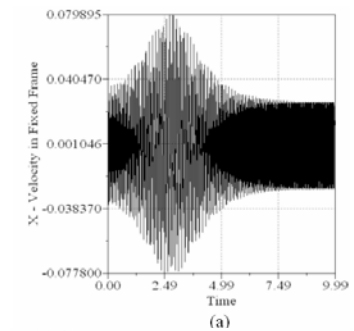


Fig 8: Dynamic response of pendulum stabilized with orbit response function-1 rotor with shaft load and eccentricity.

6 Conclusions

A single degree pendulum like rotor is considered. The spinning damping and actuation devices are assumed to be lumped in a smart coupling between the drive and the rotor.

When the rotor does not drive any load then the shaft drawn power is a good information based on which the actively contrived negative damping may be modulated to counteract the destabilizing rotating damping. It is shown the for shafts driving a load the shaft drawn power is more than the power responsible for destabilization and this to eventual instability causing the shaft to whirl in reverse direction with rapid growth whirl amplitude.

Two orbital response functions are proposed which are created by measurements of orthogonal vibration velocity amplitude in frame rotating with the shaft and the contrived negative rotating damping is modulated with these signals. It is shown that this way of damping modulation leads to extremely stable rotor even in the presence of shaft eccentricity and load.

Acknowledgment

We would like to offer a special thanks to Prof Sangram Mudali (Director NIST Berhampur) and Dr Ajit Kumar Panda (Dean NIST Berhampur) and Dr Ravi .P.Reddy (Deputy Director NIST Berhampur) for their continuous encouragement and support .

We are deeply indebted and we would like to offer our special thanks to Prof Amalendu Mukherjee (Faculty Mechanical Engineering IIT Kharagpur) for his highly valuable intellectual input throughout .

We would like to thank Dr Motehar Reza (Asst Professor NIST Berhampur) for his valuable feedback.

References

[1] N.M. Bou-Rabee, J. E. Marsden, and L. A. Romero "Dissipation-Induced Heteroclinic Orbits in Tippe Tops" SIAM Review , Vol.50, No. 2, pp 325-344. 2008,
[2] O. N. Kirillov "Gyroscopic Stabilization in the Presence of Nonconservative forces" Dokl. Math, Vol. 76, pp780-785. 2007,

[3] A. C. Or "The Dynamics of Tippe Top" SIAM J. Appl. Math. Vol. 54, pp 597-604. 1994
[4] A. K. Samantaray, R. Bhattacharyya, and A. Mukherjee "On Stability of Crandall Gyro-pendulum" Physics Letters, A 372, pp 238-243. 2008.
[5] A. Mukherjee , R. Bhattacharyya and A.M. Rao Desari " A theoretical Study of Stability of a Rigid Rotor Under the Influence of Dilute Viscoelastic Lubricants" ASME Jr. of Tribology, Vol.107, No. 1., pp 75-81, 1985.
[6] A. Harnoy. "An Analysis of Stress relaxation in Elastico-viscous Hydrodynamic Lubrication of Sleeve Bearings" ASLE Transactions , Vol 19, pp 301-308, 1976.
[7] R. Holmes " Nonlinear Performance of Squeeze Film Bearings" Jr. of Mechanical Engineering Science, Vol. 14, No. 1, pp 74-77, 1972.
[8] B. Halder, A. Mukherjee and R. Karmakar " Theoretical and Experimental Studies on Squeeze Film Stabilizer for Flexible Rotor-Bearing Systems Using Newtonian and Viscoelastic Lubricants" Jr. of Vibration and Acoustics, Transaction of ASME , Vol. 112, No. 4, pp 473-482. 1990.
[9] G. C. Tolle and D. Muster "Effect of Biphase Lubricant on Half Frequency Whirl in a Full Journal Bearing" ASME Jr. for Engineering for Industry, Nov. pp 1345-1353, 1975.
[10] A. Mukherjee " Effect of Biphase Lubricants on Dynamics of Rigid Rotors" Transaction of ASME, Jr. of Lubrication Technology, Vol. 105, pp 29-38.
[11] A. K. Samantaray, R. Bhattacharyya and A. Mukherjee. "An Investigation in to the Physics Behind the Stabilizing Effect of Two Phase Lubricants in Journal Bearings" Jr. of Vibration and Control, Vol. 12, No. 1, pp 425-442, 2006.
[12] A. Mukherjee, R. Karmakar and A. K. Samantaray " Bond Graphs in Modeling, Simulation and Fault Identification" I. K. International Publishing House Pvt. Ltd. India, CRC Taylor and Francis, USA, 2006.
[13] www.htcinfo.com (2009).